Astronomy & Astrophysics manuscript no. 3938˙a February 2, 2008
(DOI: will be inserted by hand later)

Microvariability in the optical polarization of 3C279⋆⋆⋆

I. Andruchow[1], S. A. Cellone[2], G. E. Romero[1,⋆⋆⋆], T. P. Dominici[3], Z. Abraham[3]

[1] Instituto Argentino de Radioastronomía, C.C.5, (1894) Villa Elisa, Buenos Aires, Argentina
[2] Facultad de Ciencias Astronómicas y Geofísicas UNLP, Paseo del Bosque, B1900FWA La Plata, Argentina
[3] Departamento de Astronomia, Instituto de Astronomia, Geofísica e Ciências Atmosféricas, Universidade de São Paulo, Brasil

Received / Accepted

Abstract. We present results of a microvariability polarization study in the violently variable quasar 3C279. We have resolved the polarization curves in the *V* band for this object down to timescales of minutes. We found two main components in the evolution of the degree of linear polarization, one consisting of a flicker with timescales of several tens of minutes and other component with far more significant variations on timescales of a few days. The linear polarization descended from ∼ 17 % down to ∼ 8 % in three nights. The polarization angle underwent a sudden change of more that 10 degrees in a few hours, perhaps indicating the injection of a new shock in the jet. The amplitude of the intranight flickering in the degree of polarization is at the level of ∼ 1%. These are probably the best sampled polarization data ever obtained for this object. We also performed IR observations and we provide a follow-up of the evolution of this source at such energies after the main polarization outburst.

Key words. Galaxies: active: individual: 3C279 – polarization– galaxies: photometry

1. Introduction

The blazar 3C279 ($z = 0.538$) is a strong source across the entire electromagnetic spectrum and one of the best studied extragalactic objects. Simultaneous multiwavelength observations from radio to gamma-rays (e.g. Maraschi et al. 1994; Hartman et al. 1996) show a spectral energy distribution dominated by two non-thermal contributions interpreted as synchrotron and inverse Compton radiation from relativistic electrons in the jet (e.g. Hartman et al. 2001a). The jet itself is well-resolved in multiepoch VLBI observations that allow to determine its kinematics and the evolution of the superluminal components (e.g. Carrara et al. 1993; Piner et al. 2000; Wehrle et al. 2001; Piner et al. 2003).

3C279 is extremely variable at all wavelengths. At optical bands it has shown fast and significant outbursts in a single night (e.g. Miller & Noble 1996). Rapid variations have been observed also at IR, UV, X-ray, and gamma-ray energies by many authors (e.g. Fan 1999; Pian et al. 1999; Kniffen et al. 1993; Hartman et al. 2001b). Despite these studies, very little is known about the short term polarization behaviour of this source. In this paper we present, for the first time, optical polarization curves with high temporal resolution for 3C279. We have found strong variations on timescales of days superposed on a smaller amplitude flickering of both the modulus and the angle of the *V*-band radiation polarization vector. We also present new IR observations of this blazar that shed light on the overall behaviour of the source on longer timescales.

The structure of the paper is as follows. In the next section we present a description of the polarimetric observations and the data analysis. In Section 3 we describe the main results on the polarization. Section 4 presents the infrared data. In Section 5 we discuss the origin of the observed variability. Finally, we close with the conclusions in Section 6.

2. Polarimetric observations and data analysis

The observations were made using the CASPROF polarimeter on the 2.15-m CASLEO telescope at El Leoncito, San Juan, Argentina during 4 consecutive nights, March 09–12, 2002. CASPROF was built at CASLEO, based on the designs of the previous MINIPOL and VATPOL instruments (see Magalhães et al. 1984; Martínez et al. 1990). It is a rotating plate polarimeter with a Wollaston prism that divides the incident light beam into two components, each one directed to a different photomultiplier. The instrument has an *UBVRI*-system filter wheel and a second wheel with diaphragms of different apertures. The observations were carried out using the Johnson *V* filter and the 11.3 arcsec aperture diaphragm. Weather conditions were photometric, except for the second

Send offprint requests to:

⋆ Based on observations made at the Complejo Astronómico El Leoncito, which is operated under agreement between CONICET and the National Universities of La Plata, Córdoba, and San Juan, as well as at the Laboratório Nacional de Astrofísica, LNA-CNPq, Brazil.

⋆⋆ Table 2 is available in electronic form at the CDS via anonymous ftp to cdsar.u-strasbg.fr (130.79.128.5) or via http://cdsweb.u-strasbg.fr/cgi-bin/qcat?J/A+A/.

⋆⋆⋆ Member of CONICET

night (March 10), when the observations were made through thin cirrus.

Standard stars were observed to determine the zero point for the polarization angle and the instrumental polarization (although the latter was found to be practically zero). These stars were chosen from the catalog by Turnshek et al. (1990); their parameters are given in Table 1.

Table 1. Standard stars

Name	α(2000) [h:m:s]	δ(2000) [° ′ ″]	Type	P_V [%]	θ_V [°]
HD64299	07:52:25.6	−23:17:46	zero	0.151	...
HD98161	11:17:11.8	−38:00:52	zero	0.017	...
HD298383	09:22:29.8	−52:28:57	angle	5.23	148.6
HD110984	12:46:44.9	−61:11:12	angle	5.70	91.6

In Table 2 we present polarimetric data obtained for 3C279 during our campaign. Column (1) gives the Julian Date corresponding to each observation. Columns (2) and (3) give the degree of polarization and its associated error. Columns (4) and (5) present the position angle and its error. Finally, in columns (6) and (7), we list the normalized Stokes parameters.

3. Variability results

Figure 1 presents the variation of the degree of polarization (top panel) and position angle (bottom panel) during the four nights of our campaign (time begins at UT = 0 hs on March 09, 2002). After a first glance, we can see that there are two different components in the variability with timescales of hours and days, respectively. During the first three nights, the degree of polarization drops from ∼ 17% to ∼ 8%, whereas in the last night it rises from ∼ 8% to ∼ 10%. With regard to the polarization angle, it also presents superposed variations with different timescales. In this case, however, during the first three nights the position angle shows no large-amplitude changes, remaining between 51° and 53°, while in the fourth night there is a sudden increase up to ∼ 63°.

A detailed curve for each night is given in Figure 2 *a* to *d*, where the short timescale variations can be appreciated. These can be described as a ∼ 1 % flickering in P_V and variations of up to ∼ 5 degrees in θ_V within a few tens of minutes.

After discarding a few data points affected by moonlight contamination and/or lightnings near the horizon during one night, we made two different sets of data reductions. In a first approach each data point corresponds to an individual integration. This method, however, yields large error bars. As an alternative, we averaged each pair of consecutive observations (in the $Q - U$ plane), in order to improve the statistics. General trends were similar to those obtained using the direct reduction, although the errors were smaller. The rest of our analysis is thus based on these averaged data.

Since the polarimeter measures the ordinary and extraordinary rays almost simultaneously, it is assumed that its results are immune to air transparency and seeing changes. However, a possible error source lies in the sky subtraction procedure. To measure the polarization of the radiation emitted by a source, two integrations are required: one with the object in the center of the diaphragm, and the other of the sky near the source. Then, the brightness and polarization vector for the sky are subtracted from the corresponding source observation.

Large and/or rapid variations in the sky polarization due to the presence of the Moon are expected. Since this factor affects both the object and the sky, this systematic error should be removed when the data are reduced, provided that each sky measurement is made near (both in time and position) to the corresponding source observation. The Moon was above the horizon

Table 2. Results from polarization observations of 3C279

J.D. 2452342.0+	P [%]	$\sigma(P)$ [%]	θ [°]	$\sigma(\theta)$ [°]	U/I [%]	Q/I [%]
0.68148	17.19	0.25	54.2	0.4	16.31	−5.46
0.68850	17.38	0.19	54.9	0.3	16.36	−5.88
0.69878	16.85	0.16	55.0	0.3	15.84	−5.75
0.70824	16.84	0.17	54.0	0.3	16.02	−5.20
0.71603	16.88	0.20	53.0	0.3	16.23	−4.64
0.72365	16.85	0.13	52.5	0.2	16.27	−4.37
0.73140	16.38	0.20	53.2	0.3	15.71	−4.64
0.74005	16.00	0.14	53.3	0.3	15.33	−4.58
0.74890	16.59	0.17	52.6	0.3	16.01	−4.36
0.75778	16.83	0.15	52.9	0.3	16.19	−4.60
0.76600	16.74	0.13	52.8	0.2	16.13	−4.48
0.77330	16.44	0.14	52.0	0.2	15.95	−3.95
0.78174	16.50	0.16	52.5	0.3	15.94	−4.25
0.79057	16.64	0.14	53.1	0.2	15.99	−4.63
0.79851	16.32	0.13	52.8	0.2	15.72	−4.36
0.80610	15.58	0.20	52.0	0.4	15.12	−3.76
0.81357	15.44	0.17	52.6	0.3	14.91	−4.03
0.82140	16.28	0.17	52.8	0.3	15.68	−4.37
0.82977	16.23	0.17	52.6	0.3	15.66	−4.28
0.83895	15.44	0.14	53.0	0.3	14.84	−4.26
0.84777	15.63	0.19	53.0	0.4	15.02	−4.32
0.85538	16.00	0.17	52.8	0.3	15.41	−4.31
0.86317	15.63	0.17	52.4	0.3	15.11	−4.01
0.87163	15.08	0.16	52.4	0.3	14.58	−3.84
0.87963	15.52	0.19	53.1	0.4	14.90	−4.35
1.45230	12.68	0.47	56.5	1.1	11.68	−4.93
1.62768	13.87	0.22	55.5	0.5	12.95	−4.96
1.63643	13.61	0.20	54.6	0.4	12.84	−4.49
1.64633	13.60	0.22	54.1	0.5	12.92	−4.23
1.65881	13.24	0.19	54.6	0.4	12.50	−4.34
1.66966	13.15	0.20	55.1	0.4	12.34	−4.55
1.67639	13.21	0.16	55.9	0.3	12.26	−4.92
1.68305	13.75	0.20	55.8	0.4	12.79	−5.06
1.69093	14.26	0.20	54.2	0.4	13.53	−4.50
1.69875	14.14	0.17	54.0	0.4	13.45	−4.37
1.70552	13.59	0.19	54.0	0.4	12.92	−4.20
1.71250	13.58	0.16	53.3	0.3	13.01	−3.97
1.74710	14.75	0.21	53.2	0.4	14.14	−4.17
1.78440	14.68	0.43	54.1	0.8	13.94	−4.61
1.79975	13.94	0.22	54.9	0.5	13.12	−4.71
1.81310	14.16	0.20	55.4	0.4	13.24	−5.02
1.82177	14.49	0.21	55.7	0.4	13.49	−5.28

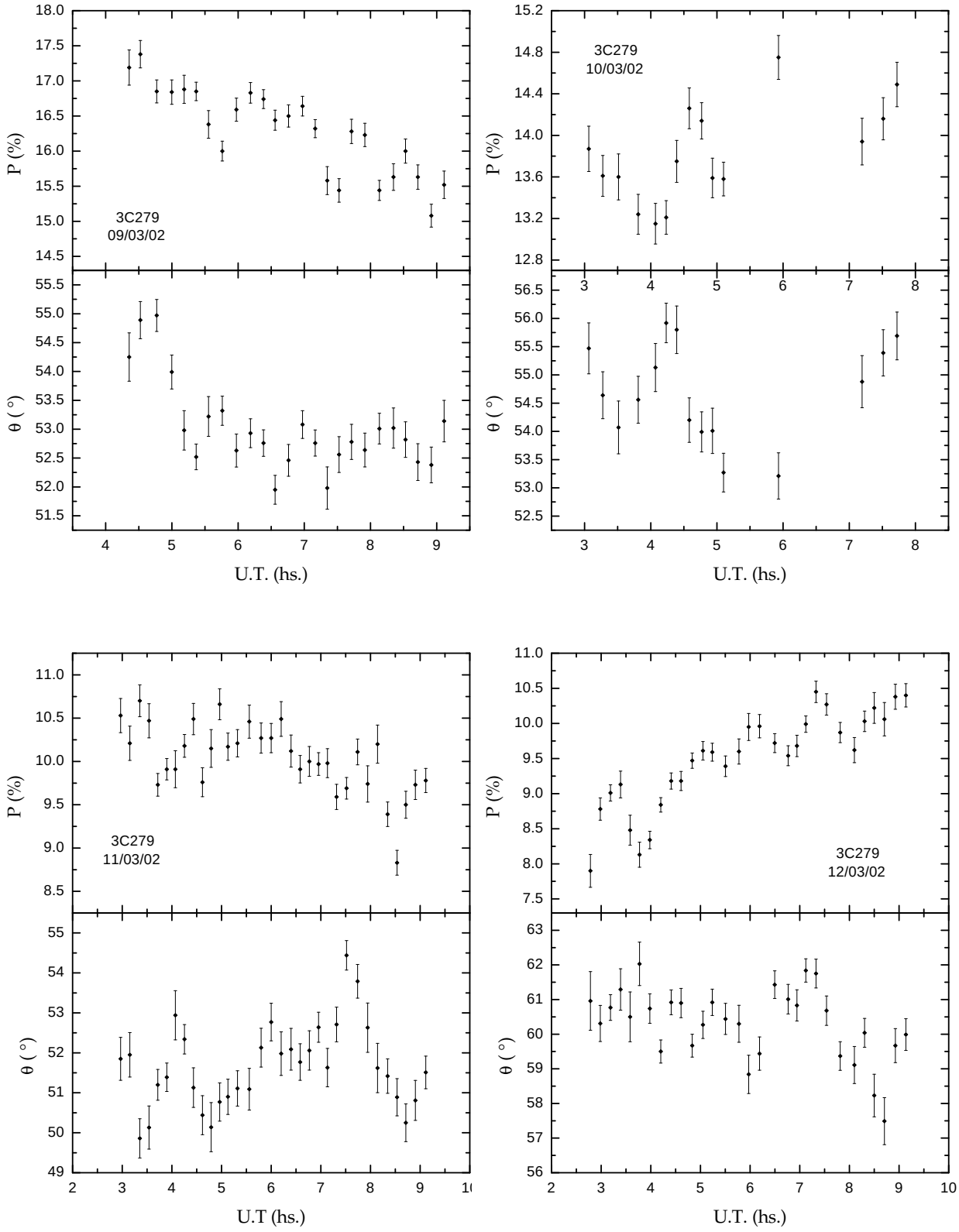

Fig. 2. A detailed view of the polarization and position angle variations for each night.

only at the end of each observing night; however, we checked for any residual systematic error by plotting the behaviour of the polarization of the object with respect to the polarization and magnitude of the sky. No spurious variation seems to be present due to this effect, neither for the polarization percentage nor for the position angle.

In order to assess whether a source presents variability from a formal and quantitative point of view, we followed the criterion of Kesteven et al. (1976) which has been used by several

Table 2. (cont.) Results from polarization observations of 3C279.

J.D. 2452342.0+	P [%]	$\sigma(P)$ [%]	θ [°]	$\sigma(\theta)$ [°]	U/I [%]	Q/I [%]
2.62362	10.53	0.20	51.8	0.5	10.23	−2.50
2.63138	10.21	0.20	52.0	0.6	9.91	−2.45
2.63971	10.70	0.18	49.9	0.5	10.55	−1.81
2.64744	10.47	0.20	50.1	0.5	10.30	−1.86
2.65481	9.73	0.13	51.2	0.4	9.50	−2.09
2.66241	9.91	0.12	51.4	0.4	9.66	−2.19
2.66962	9.91	0.21	52.9	0.6	9.53	−2.71
2.67718	10.18	0.13	52.3	0.4	9.85	−2.58
2.68476	10.49	0.18	51.1	0.5	10.25	−2.23
2.69229	9.76	0.17	50.4	0.5	9.59	−1.84
2.69962	10.15	0.22	50.1	0.6	9.99	−1.81
2.70675	10.66	0.18	50.8	0.5	10.44	−2.13
2.71373	10.17	0.16	50.9	0.4	9.96	−2.08
2.72169	10.21	0.16	51.1	0.4	9.98	−2.16
2.73165	10.46	0.19	51.1	0.5	10.22	−2.21
2.74151	10.27	0.17	52.1	0.5	9.95	−2.53
2.75000	10.27	0.17	52.8	0.5	9.90	−2.75
2.75840	10.49	0.20	52.0	0.5	10.18	−2.53
2.76667	10.12	0.19	52.1	0.5	9.81	−2.48
2.77430	9.91	0.16	51.8	0.5	9.64	−2.32
2.78202	10.00	0.17	52.1	0.5	9.70	−2.44
2.78978	9.97	0.13	52.6	0.4	9.61	−2.63
2.79725	9.98	0.17	51.6	0.5	9.71	−2.29
2.80483	9.59	0.14	52.7	0.4	9.25	−2.55
2.81320	9.69	0.13	54.4	0.4	9.17	−3.14
2.82248	10.11	0.15	53.8	0.4	9.64	−3.06
2.83100	9.74	0.21	52.6	0.6	9.40	−2.56
2.83924	10.20	0.22	51.6	0.6	9.93	−2.34
2.84774	9.39	0.14	51.4	0.4	9.16	−2.09
2.85558	8.83	0.14	50.9	0.5	8.64	−1.80
2.86303	9.50	0.16	50.3	0.5	9.34	−1.73
2.87104	9.73	0.17	50.8	0.5	9.53	−1.96
2.87969	9.78	0.14	51.5	0.4	9.53	−2.21
3.61600	7.90	0.23	61.0	0.8	6.71	−4.18
3.62431	8.78	0.16	60.3	0.5	7.55	−4.47
3.63279	9.01	0.12	60.8	0.4	7.68	−4.71
3.64130	9.13	0.19	61.3	0.6	7.70	−4.92
3.64931	8.48	0.21	60.5	0.7	7.27	−4.37
3.65723	8.13	0.18	62.0	0.2	6.74	−4.56
3.66586	8.34	0.12	60.7	0.4	7.11	−4.35
3.67504	8.84	0.10	59.5	0.3	7.73	−4.29
3.68377	9.18	0.12	60.9	0.4	7.80	−4.85
3.69201	9.18	0.14	60.9	0.4	7.80	−4.84
3.70138	9.47	0.11	59.7	0.3	8.26	−4.64
3.71044	9.61	0.13	60.3	0.4	8.28	−4.88
3.71823	9.59	0.13	60.9	0.4	8.15	−5.06
3.72931	9.39	0.15	60.4	0.4	8.06	−4.82
3.74065	9.60	0.18	60.3	0.5	8.27	−4.89
3.74885	9.95	0.19	58.8	0.6	8.81	−4.62
3.75787	9.96	0.17	59.4	0.5	8.72	−4.81
3.77062	9.72	0.14	61.4	0.4	8.16	−5.27
3.78195	9.54	0.14	61.0	0.4	8.09	−5.06
3.78927	9.68	0.15	60.8	0.5	8.24	−5.08
3.79675	9.99	0.12	61.8	0.3	8.31	−5.54
3.83752	10.45	0.15	61.7	0.4	8.71	−5.77
3.84603	10.27	0.15	60.7	0.4	8.77	−5.35
3.84695	9.87	0.14	59.4	0.4	8.66	−4.74
3.85415	9.62	0.18	59.1	0.5	8.48	−4.55
3.85585	10.03	0.15	60.0	0.4	8.68	−5.03
3.86274	10.22	0.22	58.2	0.6	9.15	−4.55
3.86730	10.06	0.24	57.5	0.7	9.12	−4.25
3.87193	10.28	0.18	59.7	0.5	9.05	−5.09

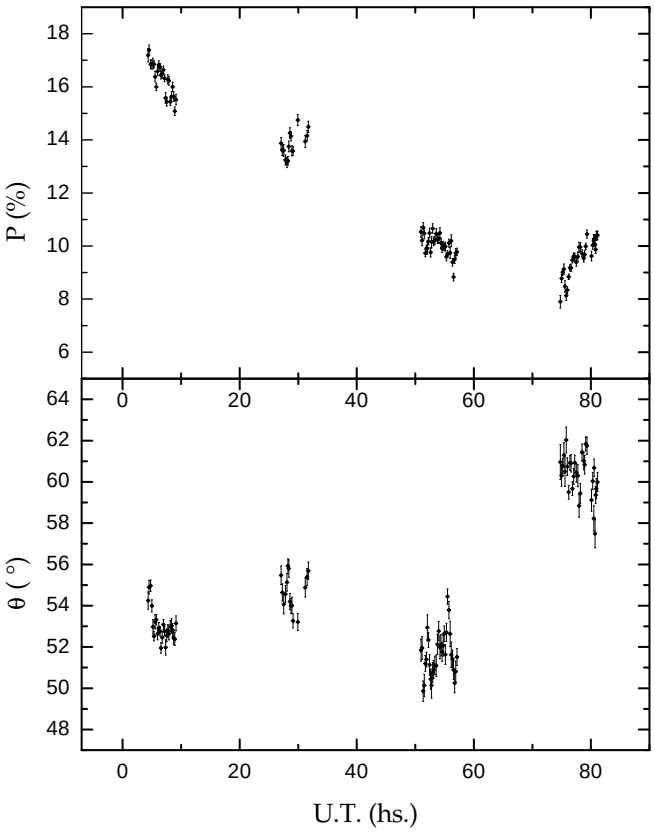

Fig. 1. Degree of polarization and position angle for the observations of 3C279 during the four nights.

authors in variability studies (Altschuler 1982; Romero et al. 1994). The variability, both in amplitude and timescale, is quantified by the following parameters: the fluctuations index μ, the fractional variability index of the source FV, and the time interval Δt between the extrema in the polarization curve. The corresponding formulae are as follows:

$$\mu = 100\frac{\sigma_{\rm s}}{\langle S\rangle}\ \%, \tag{1}$$

$$FV = \frac{S_{\rm max} - S_{\rm min}}{S_{\rm max} + S_{\rm min}}, \tag{2}$$

$$\Delta t = |t_{\rm max} - t_{\rm min}|. \tag{3}$$

Here σ_s is the standard deviation of one observation, $\langle S\rangle$ is the mean value of the polarization or the position angle measured during the observing session, $S_{\rm max}$ and $S_{\rm min}$ are, respectively, the maximum and minimum values for the polarization or the position angle, $t_{\rm max}$ and $t_{\rm min}$ are the times when the extreme points occur. Regarding the significance of the variability, a source is classified as variable if the probability of exceeding the observed value of

$$X^2 = \sum_{i=1}^{n} \epsilon_i^{-2}\,(S_i - \langle S\rangle)^2 \tag{4}$$

by chance is < 0.1 %, and non-variable if the probability is > 0.5 %. If the errors are random, X^2 should be distributed as χ^2

Table 3. Variability results for 3C279: degree of polarization

J.D.	n	μ [%]	FV	Δt [hs]	$\langle P\rangle$ [%]	χ^2	V/NV
2452342	25	3.57	0.071	4.40	16.30	308.8	V
2452343	17	3.54	0.075	3.08	13.78	91.0	V
2452344	33	4.02	0.096	5.18	9.97	196.2	V
2452345	30	6.48	0.139	4.54	9.47	503.4	V
All	103	72.77	0.375	70.26	11.68	33554.7	V

Table 4. Variability results for 3C279: position angle

J.D.	n	μ [%]	FV	Δt [hs]	$\langle\theta\rangle$ [°]	χ^2	V/NV
2452342	25	1.38	0.028	1.79	53.0	157.0	V
2452343	17	1.69	0.030	3.08	54.7	75.5	V
2452344	33	2.10	0.044	4.21	51.7	174.1	V
2452345	30	1.54	0.138	4.93	60.4	126.3	V
All	103	20.32	0.109	24.42	54.5	7721.9	V

whit $n-1$ degrees of freedom, where n is the number of points in the distribution.

In Tables 3 and 4 we show the values of the variability parameters for the polarization percentage and the position angle, respectively. Column 1 gives the Julian Date, Column 2, the number of points for each night, Column 3 presents the value of μ, Column 4, FV, Column 5, Δt, Column 6 gives the mean polarization (mean angle) for each night, Column 7, the value of χ^2, and Column 8 shows the variability class (V: if the source is variable, NV: if it is not variable). The last row in each table shows values for the whole four nights observing run.

3.1. Stokes parameters

An alternative way to present the results is through the Stokes parameters. We shall consider, as usual, normalized dimensionless parameters U/I and Q/I.

In Figure 3, we present the 3C279 data in the $U/I - Q/I$ plane for the whole campaign. We can describe this pattern like a random walk in this space. Figures 4 *a* to *d* show details for each night. In this expanded view we can also see that there is no systematic pattern in the $Q-U$ plane, suggesting a chaotic (turbulent) origin for the phenomenon.

3.2. Visual Magnitude

Additional information is provided by the visual magnitude of the source, which was obtained simultaneously to each polarimetric measurement. However, the intranight trend in the V magnitude is within the expected variations due to instrumental and atmospheric errors. In any case, no strong correlation with the observed variations in polarization degree and position angle is clearly evident.

On the other hand, there is a hint for an inter-night magnitude variation. We calculated the mean value of m_V for each night and for the whole campaign. These mean values for the photometric nights are as follows: first night, $\langle m_V\rangle = 15.0$; third night, $\langle m_V\rangle = 15.1$; last night, $\langle m_V\rangle = 15.1$; then the source dimmed by 0.1 mag. at the V band during the four nights. Our mean magnitudes for 3C279 are thus consistent with those obtained by Shrader et al. (1994) during an outburst occurred in June 1992.

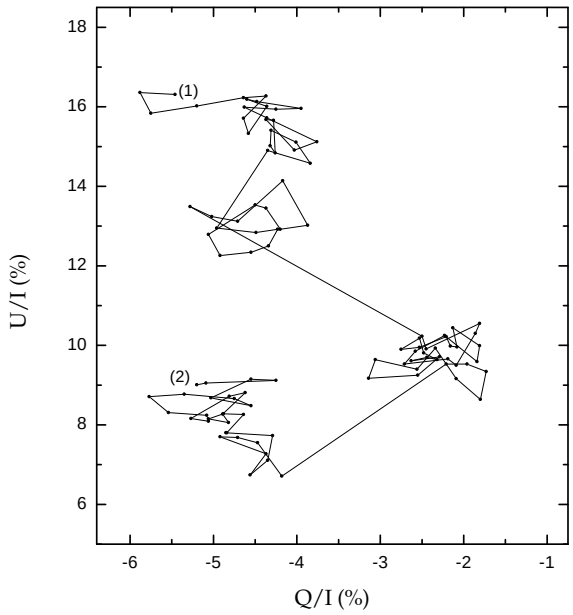

Fig. 3. Normalized Stokes parameters for 3C279 (entire campaign). (1) indicates the initial data point, and (2) is the final one.

4. Infrared observations

The data in the near-infrared range (J and H filters) were taken with the 1.6-m telescope at the LNA (Laboratório Nacional de Astrofísica, Brazópolis, Brazil), using the CamIV, an infrared camera with a HAWAII 1024×1024 pixel HgCdTe detector (18.5 μm pixel^{-1}). The field of the resulting frames has 4 arcmin on each side, with a scale of 0.24 arcsec pixel^{-1}. We obtained two frames of 120 seconds of total integration time each, with one arcmin offset between them, to subtract the emission from the sky. Because of the poor weather conditions, the observations were made only for a few hours in the nights of March 9 and 11, 2002. Hence, a full lightcurve for the entire period covered by the polarimetric campaign is not available, unfortunately.

The reduction of the near infrared observations was made with the IRAF[1] tasks developed for the CamIV data analysis

[1] IRAF is distributed by the National Optical Astronomy Observatories, which are operated by the Association of Universities

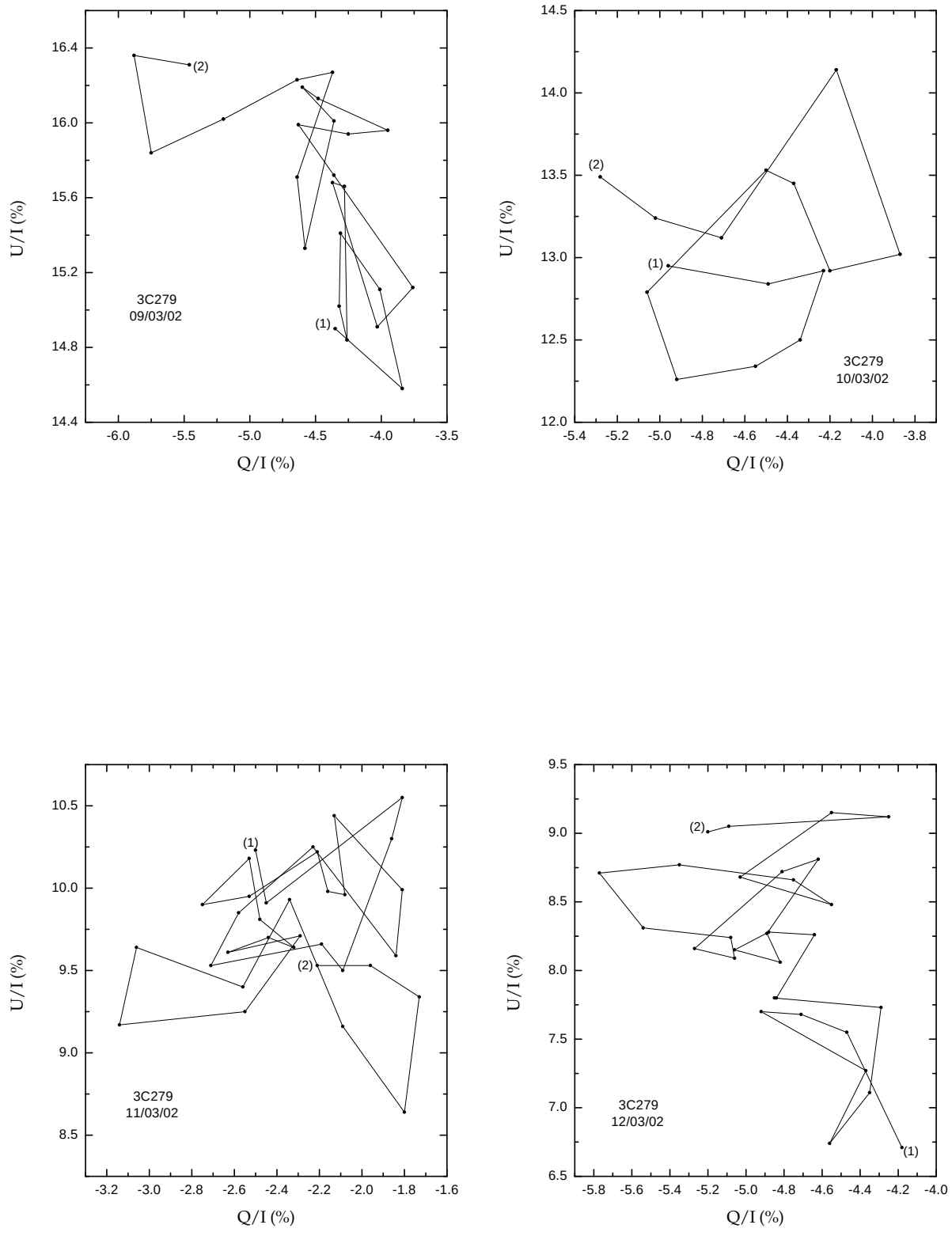

Fig. 4. Stokes parameters for each night. Again, (1) and (2) indicate the initial and final data point in each case.

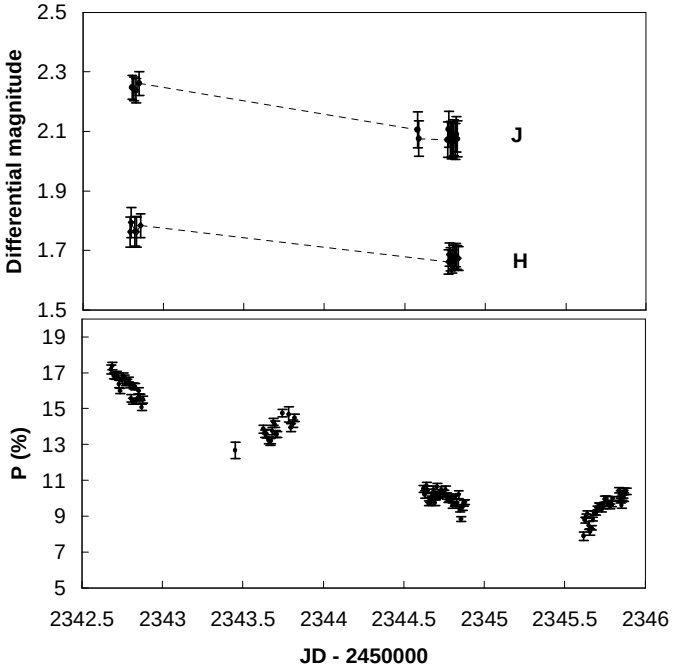

Fig. 5. Upper panel: Differential light curve of 3C279 in the *J* and *H* filters (comparison - target). **Lower panel:** Optical *V* band polarization

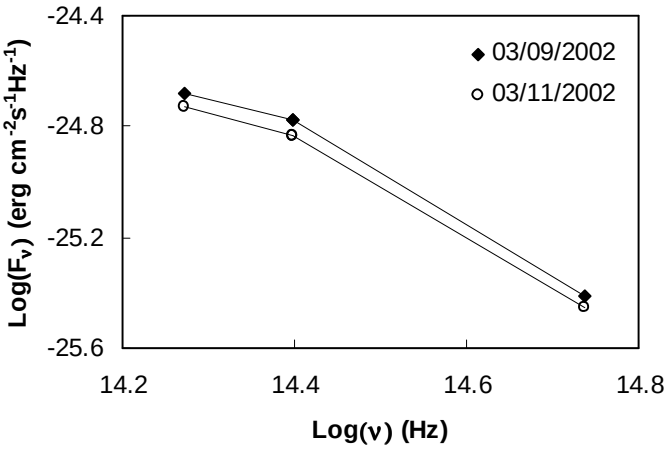

Fig. 6. Spectral behavior in the nights of March 9 and March 11, showing the flux decrease and that the mechanism that are causing the variations (polarization and continuum flux) do not cause changes in the spectral indices.

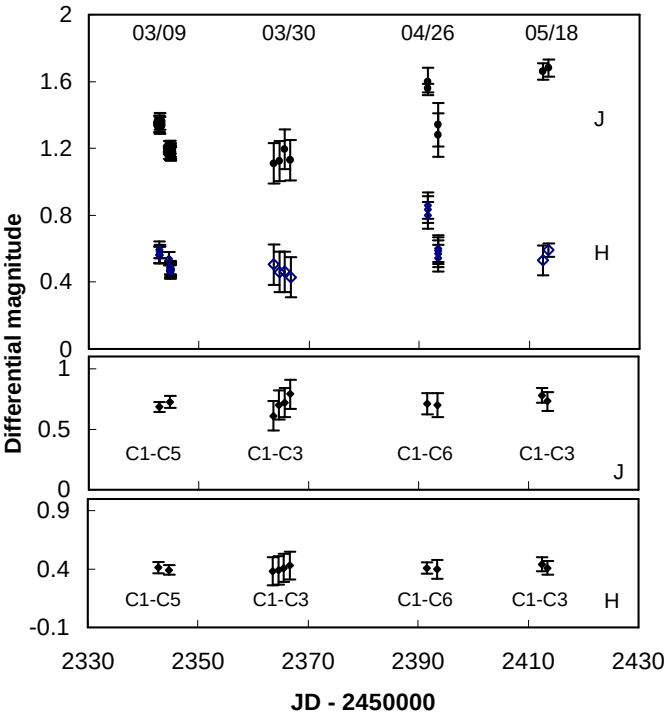

Fig. 7. Differential light curve of 3C279 in the *J* and *H* filters during ten nights of observations in 2002, divided in four campaigns between March 9 and May 19.

by F. Jablonski (private communication, 2001). The two offset frames were combined after correcting them by flat field, dark contribution and possible bad pixels in the detector. The instrumental magnitudes were calculated using the APPHOT task for aperture photometry, with an aperture of three or four times the FWHM.

The lightcurves were constructed in differential mode, with different field stars of similar magnitude to the object used for control and comparison purposes (see Cellone et al. 2000, for a detailed discussion of the procedure). The fluctuations in the lightcurves that could be interpreted as intranight variations are within the estimated errors. However, a brightness decrease between the two nights could be observed, amounting to 0.13 mag in *J* and 0.19 mag in *H*. The differential lightcurves can be seen in Figure 5, where the error bars correspond to the dispersion of the control lightcurve. 3C279 is the only object in the field to show this inter-night variation, which guarantees the confidence of the detection. It is interesting to notice that the general trend of the infrared variability mimics the behaviour of the degree of polarization, with a qualitatively similar decrease.

The variability criterion adopted is the one used by Jang & Miller (1997), Romero et al. (1999), and others: we calculated a parameter $C = \sigma_T/\sigma$, where σ_T is the standard deviation of the target differential lightcurve and σ is the standard deviation of the control lightcurve. A source can be classified as variable with 99% confidence level if $C \geq 2.576$. The analysis for data taken with both filters in the infrared yields that the source formally classifies as non-variable at all timescales except for averaged values from night to night. Stars from Persson et al. (1998) were observed for flux calibration and spectral index calculation. After correction for redenning, we found that the near-infrared spectral index remained constant in these two nights, as shown in Figure 6, with $\alpha_{ir} = -0.80 \pm 0.01$ (considering $F_\nu \propto \nu^\alpha$).

Since at the final of the coordinated campaign 3C279 showed an increase in the degree of polarization as well as a sudden change in the polarization angle, we decided to follow up its near-infrared behavior in the subsequent months. The observations were carried out with the CamIV installed in the 0.6-m B&C telescope at LNA (field of view of 8' x 8', with 0.47

for Research in Astronomy, Inc., under cooperative agreement with the National Science Foundation.

arcsec pixel^{-1} resolution) for about one hour per night in three campaigns during March 30 to April 2, April 26 and 29, and May 18-19. The resulting light curves in *J* and *H* bands can be seen in Figure 7, which includes the first two nights (March, 9 and 11) observation. The control light curves are also shown for the two filters. The stars used for comparison were not the same for all campaigns. As we already described above, in the first observing run we used the 1.6 m telescope, with a small field of view. In the subsequent campaign, the 0.6 m telescope was used and the larger field allowed the use of a better sampled star. The star chosen in campaigns 2 and 4 were not in the field in campaign 3, and for that reason, a third comparison was used. In the figure, the C1-C5 and C1-C6 control light curves were arbitrarily shifted in relation to C1-C3 for better visualization. Finding charts with the indications of the reference and control stars are available upon request. The maximum brightness variation of 3C279 detected in long time scales was about 0.4 magnitudes in the two filters, between March 10 and April 29. In time scales of days, the object infrared brightness decreased by 0.3 magnitudes between April 26 and 29.

In general, the behavior of *J* and *H* light curves was similar, except in May, 2002, when the *J* magnitudes increased in 0.3 magnitudes relative to its value is April 29, while the H magnitude did not vary in the same period. This behavior was not observed in the control light curves, which indicates that it must be real.

5. Discussion

The polarized optical emission is expected to be synchrotron radiation originated in the relativistic jet of 3C279. The rapid variability, with timescales from minutes to hours, seems to favor models based on the interaction of a relativistic shock with some obstacles along the inner jet (e.g. Gopal-Krishna & Wiita 1992).

Small variations in the direction of the shocks that propagate down the relativistic jet can produce large variations in the observed flux and polarization. Recent evidence for changes in the trajectory of superluminal components in 3C279 has been found by Homan et al. (2003) at kpc-scales. These changes can be quite frequent in the turbulent environment of the inner pc-scale jet.

The fractional polarization of the shock as a function of the angle with the line-of-sight affected by the relativistic aberration, θ', the compression factor of the plasma, k, and the spectral index, α, is (Hughes et al. 1985, e.g.):

$$\Pi = \frac{1-\alpha}{5/3-\alpha}\ \frac{(1-k^2)\sin^2\theta'}{2-(1-k^2)\sin^2\theta'}. \quad (5)$$

The relation between θ' and the actual viewing angle, θ, is given by:

$$\cos\theta' = \frac{\cos\theta-\beta}{1-\beta\cos\theta}, \quad (6)$$

where $\beta = (1-\Gamma^{-2})^{1/2}$ is the relativistic velocity of the shock and Γ is the Lorentz factor of the shocked plasma.

In the case of a perpendicular, relativistic strong shock, the factor by which the jet plasma is compressed by the shock, k, can be written as (Blandford & McKee 1976):

$$k^{-1} = \frac{n_{\rm ps}}{n_{\rm j}} = \frac{\hat{\gamma}\Gamma_{\rm ps}+1}{\hat{\gamma}-1}. \quad (7)$$

In this expression, $n_{\rm ps}$ and $n_{\rm j}$ are the particle densities in the shocked gas and in the underlying jet, respectively, $\hat{\gamma}$ is the adiabatic index, which has a value $\hat{\gamma} = 13/9$ for a gas with equal fractions of relativistic electrons and non-relativistic protons, and $\Gamma_{\rm ps}$ is the Lorentz factor of the shocked gas measured in the frame of the unshocked gas. If we take the same velocity for the shock and the shocked plasma in order to simplify the equations, $\Gamma_{\rm ps}$ can be expressed as (see Romero et al. 1995):

$$\Gamma_{\rm ps} \simeq \frac{\Gamma\gamma_{\rm j}(1-\beta^2)}{\sqrt{2}}. \quad (8)$$

Here $\gamma_{\rm j}$ is the Lorentz factor of the underlying jet. Since the superluminal components are expected to be extremely relativistic even respect to the jet, we adopt a mild value $\gamma_{\rm j} \sim 2$ for the stable, underlying flow (Marscher & Gear 1985; Romero et al. 1995).

In the particular case of 3C279, we assume an average value of $\alpha = -0.95$ for the spectral index at optical wavelengths (de Pater & Perley 1983). Concerning the Lorentz factor, we adopt as an average value the result of the fit of superluminal components with the precessing jet model proposed by Abraham & Carrara (1998). This model yields $\Gamma = 13$ for $H_0 = 70$ km s^{-1} Mpc^{-1}. We consider values of Γ of 8, 12, 13 and 16. The aberrated viewing angle at the present epoch is $\theta' \sim 26$ deg, which is in good agreement with the value given by Piner et al. (2003), once the aberration is corrected (i.e. $\theta \sim 2$ deg).

In Figure 8 we show the evolution of the fractional polarization in the observer system with the viewing angle. The angle is corrected for aberration. In the zoom-in panel we show the detail of the changes for small viewing angles as expected for 3C279. It can be seen that just a small change in the orientation of the shock velocity can produce a large change in the degree of polarization. In order to get a rapid variation of ~ 10 % as we observed, a change of ~ 2 deg is enough. The dependence on Γ is not very strong for small angles. A deviation of the shock on small timescales can be the effect of an helical magnetic field produced by the jet precession (Roland et al. 1994).

Alternatively to the purely kinematic model of Gopal-Krishna & Wiita (1992), rapid changes in the polarization might result from turbulent effects that introduce rapid changes in the compression factor k (Marscher 1992). In Figure 9 we show the fractional polarization Π as a function of k for different aberrated viewing angles. From the figure it is clear that even very strong variations in k cannot produce large changes in Π. Hence we favor a kinematic model with a changing viewing angle as the best explanation for the observed behaviour of the polarization at internight timescales. Nonetheless, the rapid intranight flickering can be the effect of turbulence (and the consequent fluctuation of the compression ratio) in the post-shock region.

Table 5. Results for the infrared observations of 3C279

Filter	J.D.	σ	Δt [hs]	C	V/NV
J	2452342	0.010	1.1	0.28	NV
J	2452344	0.014	6.0	0.32	NV
H	2452342	0.014	1.5	0.28	NV
H	2452344	0.022	6.0	0.50	NV

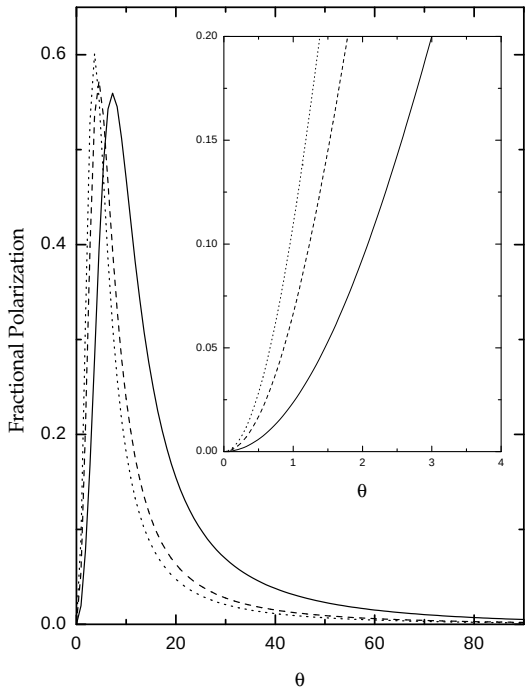

Fig. 8. Variation of the fractional polarization as a function c the angle with the line-of-sight. The solid line is for $\Gamma = 8$, th dashed one is for $\Gamma = 12$ and $\Gamma = 13$, and the dots line is fc $\Gamma = 16$. The zoom-in panel shows a detail of the same plot a low values of θ.

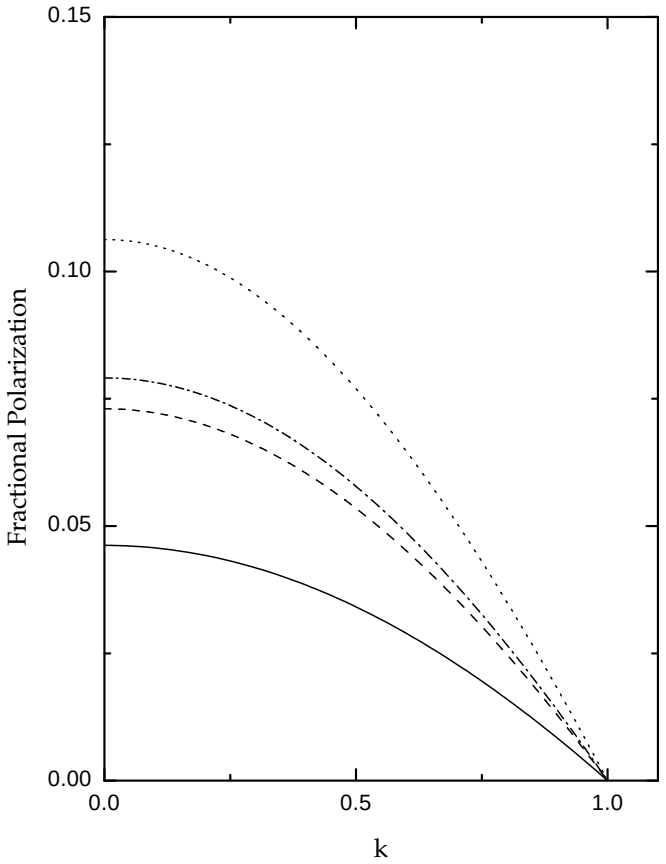

Fig. 9. Variation of the fractional polarization as a function of the factor of compression of the plasma. The solid line is for $\theta' = 20°$, the dashed one is for $\theta' = 25°$, the dash-dots line is for $\theta' = 26°$, and the dots are for $\theta' = 30°$.

The sudden change in the polarization angle observed between the nights of March 11 and 12, 2002, might be the result of the injection of a new shock in the jet. The shock compresses the magnetic field parallel to the shock front producing a sudden change in the position angle of the polarized synchrotron flux. The infrared observations show a decrease of the flux that accompanies the decrease in the degree of polarization. If a new shock was injected in early March 12, then the flux should have raised afterwards. Unfortunately, due to the weather conditions, no observations were possible that night at LNA Observatory. However, the achromatic 0.4 magnitudes variation in the near infrared flux 0.4 magnitudes observed in April, 26 and the chromatic variations in May 18-19, are compatible with short lived shocks, with relatively high formation rates.

6. Conclusions

We have carried out polarization observations with very high time resolution of the OVV blazar 3C279. A large variation of $\sim$ 10% in the degree of linear polarization was observed on internight timescales. More rapid flickering, with timescales from minutes to hours, was also present within each single night. Simultaneous infrared observations indicate that the total synchrotron flux was decreasing while the fractional polarization was also decreasing. This overall behaviour and IR observations on larger time scales seems to agree with what is expected from a relativistic shock that changes mildly the viewing angle. The rapid flickering might be due to turbulence in the post-shock region. New simultaneous multiwavelength and polarization observations of this extremely active source can

shed further light on the interactions of relativistic shocks with small features or bends in the inner jet.

Acknowledgements. Research on AGNs with G.E Romero is mainly supported by Fundación Antorchas. Additional support was provided by the Agencies CONICET (PIP 0430/98) and ANPCT (PICT 98 No. 03-04881). GER thanks the kind hospitality of the Max-Planck-Institut für Kernphysik (Heidelberg) where the final part of this work was completed. TPD and ZA acknowledges FAPESP support (98/07491-8 and 00/06769-4) and CNPq (306062/88). We thank constructive comments by Dr. L. Takalo.

References

Abraham, Z. & Carrara, E. A. 1998, ApJ, 496, 172
Altschuler, D. R. 1982, AJ, 87, 387
Blandford, R. D. & McKee, C. F. 1976, Physics of Fluids, 19, 1130
Carrara, E. A., Abraham, Z., Unwin, S. C., & Zensus, J. A. 1993, A&A, 279, 83
Cellone, S. A., Romero, G. E., & Combi, J. A. 2000, AJ, 119, 1534
de Pater, I. & Perley, R. A. 1983, ApJ, 273, 64
Fan, J. H. 1999, MNRAS, 308, 1032
Gopal-Krishna & Wiita, P. J. 1992, A&A, 259, 109
Hartman, R. C., Böttcher, M., Aldering, G., et al. 2001a, ApJ, 553, 683
Hartman, R. C., Villata, M., Balonek, T. J., et al. 2001b, ApJ, 558, 583
Hartman, R. C., Webb, J. R., Marscher, A. P., et al. 1996, ApJ, 461, 698
Homan, D. C., Lister, M. L., Kellermann, K. I., et al. 2003, ApJ, (in prees)
Hughes, P. A., Aller, H. D., & Aller, M. F. 1985, ApJ, 298, 301
Jang, M. & Miller, H. R. 1997, AJ, 114, 565
Kesteven, M. J. L., Bridle, A. H., & Brandie, G. W. 1976, AJ, 81, 919
Kniffen, D. A., Bertsch, D. L., Fichtel, C. E., et al. 1993, ApJ, 411, 133
Magalhães, A. M., Benedetti, E., & Roland, E. H. 1984, PASP, 96, 383
Maraschi, L., Grandi, P., Urry, C. M., et al. 1994, ApJ, 435, L91
Marscher, A. P. 1992, in Physics of Active Galactic Nuclei, ed. J. A. Zensus & S. J. Wagner (Heidelberg: Springer-Verlag), 510
Marscher, A. P. & Gear, W. K. 1985, ApJ, 298, 114
Martínez, E., Aballay, J. L., Marún, A., & Ruartes, H. 1990, Bol. Asoc. Arg. de Astronomía, 36, 342
Miller, H. R. & Noble, J. C. 1996, in ASP Conf. Ser. 110: Blazar Continuum Variability, 17
Persson, S. E., Murphy, D. C.and Krzeminski, W., M., R., & Rieke, M. 1998, AJ, 116, 2475
Pian, E., Urry, C. M., Maraschi, L., et al. 1999, ApJ, 521, 112
Piner, B. G., Edwards, P. G., Wehrle, A. E., et al. 2000, ApJ, 537, 91
Piner, B. G., Unwin, S. C., Wehrle, A. E., et al. 2003, ApJ, in press
Roland, J., Teyssier, R., & Roos, N. 1994, A&A, 290, 357
Romero, G. E., Cellone, S. A., & Combi, J. A. 1999, A&AS, 135, 477
Romero, G. E., Combi, J. A., & Colomb, F. R. 1994, A&A, 288, 731
Romero, G. E., Combi, J. A., & Vucetich, H. 1995, Ap&SS, 225, 183
Shrader, C. R., Webb, J. R., Balonek, T. J., et al. 1994, AJ, 107, 904
Turnshek, D. A., Bohlin, R. C., Williamson, R. L., et al. 1990, AJ, 99, 1243
Wehrle, A. E., Piner, B. G., Unwin, S. C., et al. 2001, ApJS, 133, 297